Supporting Information

Injured liver-released miRNA-122 elicits acute pulmonary inflammation via activating alveolar macrophage TLR7 signalling pathway

Yanbo Wang[1*], Hongwei Liang[1,2*], Fangfang Jin[3*], Xin Yan[4*], Guifang Xu[5], Huanhuan Hu[1], Gaoli Liang[1], Shoubin Zhan[1], Xiuting Hu[1], Quan Zhao[1], Yuan Liu[2], Zhen-You Jiang[6], Chen-Yu Zhang[1¶], Xi Chen[1¶], and Ke Zen[1¶]

File list:

Materials and Methods

Animal and model construction

C57Bl/6J and SCID (severe combined immune deficiency) mice were purchased from the Model Animal Research Center, Nanjing University (Nanjing, China). TLR7-KO mice were obtained from The Jackson Laboratory (Bar Harbor, Maine, USA) and all the knockout mice were backcrossed with C57BL/6 mice over ten generations (1). All mouse protocols followed the National Institutes of Health guide for the care and use of mice and were approved by IACUC, Nanjing University (Nanjing, China). To construct the mouse acute liver injury model, C57BL/6 mice (8-10 weeks) were intravenously injected with 5 mg/kg ConA (2) and sacrificed after 6 h. Chronic hepatic damage was induced by intraperitoneal injection of DEN (3) into mice every week for 4 weeks (100 mg/kg). To build the HCC model, HepG2 cells (1×10^6) were slowly injected into the livers of 8-week-old male SCID mice (nu/nu) (4), the mice were sacrificed 5 weeks later after the injection.

Cells

RAW264.7 macrophages was purchased from Shanghai Institute of Cell Biology, Chinese Academy of Sciences (Shanghai, China) and cultured in DMEM supplemented with 10% foetal bovine serum (GIBCO, CA, USA). Cells in BAL were isolated as previously described (5). Briefly, male C57BL/6J mice (6-8 weeks old, 20-22g) were anaesthetized with intraperitoneal pentobarbital and sacrificed by means of exsanguination. Mouse lungs were lavaged through an intratracheal catheter with pre-warmed PBS supplemented with 0.6 mmol/L EDTA, a total of 5 mL was used in each mouse. Lavage fluids were pooled and centrifuged at 300 ×g for 10 minutes to collect the cells. For peritoneal macrophage isolation, mice were administered 3% sterile thioglycollate intraperitoneally to isolate peritoneal macrophages. After resting for 6 days, the mice were sacrificed, and peritoneal lavage was performed using 10 mL of RPMI 1640 (Invitrogen, Carlsbad, CA, USA). The lavage fluid was centrifuged at 300 ×g for 10 minutes to collect the cells. To purify macrophages and epithelial cells from lung tissues (6), tissues were collected, cut into small pieces, and incubated in dissociation solution comprising 2 mg/ml collagenase type I, 2 mg/ml collagenase type IV, and 1 mg/ml DNase (all from Sigma). The solutions were pipetted every 10 min during the incubation, and suspensions were dispersed through a 70-μm cell strainer. Macrophages ($CD45^+F4/80^+$) and

epithelial cells ($CD45^{-}Epcam^{+}$) were sorted using a BD FACS Aria II SORP with purities > 95%. Primary hepatocyte were isolated as previously described (7). All cells were incubated at 5% CO_2 and 37℃ in a water-saturated atmosphere.

Histopathological examination

Histological analysis of lung sections was performed with H&E staining as previously described (8), and the sections were examined semi-quantitatively by scoring 5 parameters: pulmonary oedema, inflammatory infiltration, atelectasis, haemorrhage and hyaline membrane formation. The scores ranged as follows: 0, no injury; 1, < 25% injured; 2, 25% to 50% injured; 3, 50% to 75% injured; and 4, > 75% injured. Ten high-magnitude fields from each slide were analysed, and data are presented as the mean ± SEM.

Flow cytometry and cell sorting

Total BAL cells were washed in buffer (10 mM Hepes, 150 mM NaCl, 2.5 mM $CaCl_2$), incubated with the respective primary and secondary mAbs, and evaluated on a BD FACScalibur device and analysed with FCS express V3 FACS as previously described (9). The following antibodies were used: PE-conjugated anti-mouse CD45, FITC-conjugated CD11b and CD11c and APC-conjugated F4/80 (eBioscience, San Diego, CA, USA).

ELISA assays

Cytokine levels from BALF were analysed using ELISA kits (R&D Systems, Minneapolis, MN, USA) following the manufacturer's instructions (9).

RNA isolation and quantitative RT-PCR

Total RNA was extracted using TRIzol Reagent (Invitrogen) according to the manufacturer's instructions. Stem-loop RT-qPCR assays using TaqMan miRNA probes (Applied Biosystems, Carlsbad, CA, USA) were performed to quantify the levels of mature miRNAs as described previously (4). To quantify mRNA, 1 μg of total RNA was reverse-transcribed into cDNA using oligo dT and Thermoscript (TaKaRa, Dalian, China) and sequentially

incubated at 16 ℃ for 30 min, 42 ℃ for 30 min and 85 ℃ for 5 min. To test pre-miR-122 expression, reverse transcription PCR and real-time PCR were performed. All the primer sequences are listed in SI Appendix, Tables S3. In specific, total RNA was isolated from the plasma samples using a 1-step phenol/chloroform purification protocol as previously described (10). To calculate the absolute expression levels of miR-122 in plasma, synthetic miR-122 oligonucleotides at known concentrations were detected to construct a standard curve (11). The absolute amount of miR-122 in plasma was then calculated in reference to the standard curve.

Exosome isolation

Exosomes were isolated from the plasma and cell culture medium via differential centrifugation as previously described (12). Briefly, after discarding off cells debris by centrifugation at 300 × g, 1200 ×g, and 10,000 × g, the supernatant was centrifuged at 110,000 × g for 70 min (all of these steps were performed at 4 ℃). The exosomes were collected from the pellet and resuspended in PBS.

Depletion of miR-122 in plasma collected from ConA-treated mice

Plasma samples were collected from ConA-treated mice, and miR-122 depletion was performed as described previously (13). Biotin-anti-miR-122 complementary to human mature miR-122 (sequence: 5'-ACAAACACCAT TGTCACACTCCAA-3') was synthesized (Genscript, Nanjing, China), 3'- and 5'-labelled with biotin and dissolved in buffer (500 mM NaCl, 20 mM Tris-HCl and 1 mM EDTA, pH7.5) at a final concentration of 20 pmol/ml. Biotin-anti-miR-122 was then incubated with streptavidin-coated magnetic beads (Cat. S1420S, New England BioLabs, Ipswich, MA, USA) according to the manufacturer's instructions (13). Plasma samples were pre-treated with DNase I (Takara) and then incubated with biotin-anti-miR-122-coated magnetic beads at 37 ℃ for 1 h. Magnets were applied to attract the beads, and the supernatants were collected. This process was repeated once more, and the collected supernatants were used for adoptive transfer experiments.

Adoptive transfer of plasma

Briefly, 200μl plasma samples from control mice (Normal), ConA-treated mice (ConA) and ConA-treated mice after plasma miR-122 depletion ($ConA^{-miR-122}$) were separately injected into WT mice via tail vein (6 mice/group) for six times (one injection every 6 h); the mice were sacrificed 3 h later after the final injection.

Efficient inhibition of miR-122 in mice liver using rAAV vectors

The AAV-anti-MiR122 TuD constructs were generated as previously described (14). Briefly, the chemically synthesized miR-122 sponge sequence flanked with *XbaI* and *ApaI* sites was digested and cloned into the *XbaI*–*ApaI* polylinker of pGL3 to create SV40 promoter–driven miR-122 sponge expression cassettes. Then, the fragment containing miR-122 sponge was isolated by *NcoI* and *ApaI* double digestions from pGL3 miR-122 sponge and cloned into the *KpnI* site of pAAVCBPI plasmid or between *PstI* and *MluI* sites of pAAVTBGPI plasmid to generate CB and TBG promoter–driven sponge expression vectors, respectively. Six-week-old C57BL/6J male mice were treated by tail vein injection with AAV vectors at 1×10^{12} genome copies/mouse.

Direct injection of miR-122 or miR-122-mut via the tail vein or respiratory trachea

For tail vein injection, 10 nmol of synthetic miR-122, miR-122-Cy5 (5'-end) or miR-122-mut (Takara) was dissolved in 150μl of PBS and then injected via the tail vein. For trachea injection, 5 nmol of synthetic miR-122, miR-122-Cy5 or miR-122-mut was dissolved in 100μl of PBS and then injected into mouse lungs via the respiratory trachea, the mice were sacrificed 6 h later.

Immunofluorescence and immunohistochemistry staining

Immunofluorescence was performed as described previously (15). Primary antibodies against TLR7 (1:200, NBP2-24906, Novus Biologicals, Littleton, CO, USA) and F4/80 (1:100, MAB5580, R&D systems) were used, and DAPI (Santa Cruz Biotechnology, Santa Cruz, CA, USA) was used for nuclei staining. For co-localization analysis of TLR7 and miR-122, RAW264.7 cells were seeded into 24-well plates for 12 h to 50% confluence. Cells were then treated with mature miR-122-Cy5, washed three times with PBS and incubated for 30 min with LysoTracker Blue DND-22 (Invitrogen) diluted 1:25,000 in PBS. After incubation with TLR7 primary antibody and appropriate

secondary antibody, the cells were analysed under a confocal microscope. To evaluate liver inflammatory forms of cell death, liver sections were processed for immunohistochemical staining as previously described (4). Using a microwave-based antigen retrieval technique, specimen slides were incubated overnight at 4℃ with primary antibodies against cleaved caspase-3 (19677-1-AP, Proteintech, Wuhan, China), RIP3 (#95702, Cell Signalling Technology, Danvers, MA, USA) or cleaved caspase-1 (#4199, Cell Signalling Technology).

Apoptosis, necroptosis and pyroptosis induction

Apoptosis and necroptosis was induced as described previously (16). Briefly, apoptosis was induced by TNF-α (30 ng/ml) and Smac (10 nM) for the indicated time periods. Necroptosis was induced by z-VAD-fmk (20μM), Smac mimetic (10 nM) or cycloheximide (10μg/ml) (MedChemExpress, Monmouth Junction, NJ, USA) for 30 min and followed by TNF-α (30 ng/ml) for the indicated time periods. Pyroptosis was induced as described previously (17). Briefly, LPS, lipid A or the control agonists (MDP and Pam3CSK4) were electroporated into indicated cells using the Neon Transfection System (Life Technologies, Carlsbad, CA, USA) following the manufacturer's instructions.

Macrophage depletion

For macrophage deletion, mice were pretreated with clondroate liposomes (200μl/mouse, obtained from Nico van Rooijen, Vrije Universiteit, Amsterdam, Netherlands) as previously described (18, 19), 2 days prior to ConA or synthetic miR-122 injection.

Co-immunoprecipitation

RAW264.7 cells were treated with the indicated miRNAs for 20 min at 37℃. Cells were then extensively washed with ice-cold PBS, collected and lysed with 150μl of lysis buffer (20 mM Tris-HCl, 150 mM NaCl, 0.5% Nonidet P-40, 2 mM EDTA, 0.5 mM DTT, 1 mM NaF, 1 mM PMSF and 1% Protease Inhibitor Cocktail (Sigma), pH 7.5) as previously described (13). Lysates were harvested at 16,000g (10 min, 4℃) and immunoprecipitated with a rabbit anti-TLR7 antibody or normal IgG followed by protein G sepharose beads. After elution from the beads, RNA was extracted with TRIzol and subjected to real-time analysis.

Western blotting

Protein levels were analysed via Western blotting using selective antibodies and normalized to GAPDH. The following antibodies were used: anti-TLR7 (H-6, Novus Biologicals) and anti-GAPDH (sc-365062, Santa Cruz Biotechnology). Protein bands were analysed using Image J software.

***In situ* hybridization**

In situ hybridization of mouse lung tissues was performed using an LNA probe directed against mmu-miR-122 (5′-CAAACACCATTGTCACACTCC-3′) synthesized by Exiqon as described previously (15).

Transcript microarray profiling

RAW264.7 macrophages were stimulated with synthetic miR-122 for 6 h and then used for mRNA isolation. Microarrays were performed using Whole Mouse Genome Microarray 4X44K v2 (Agilent Technologies, Palo Alto, CA, USA). Briefly, labelled cDNA was synthesized using the Quick Amp Labelling kit and hybridized with Agilent SureHyb. Slides were scanned with an Agilent DNA Microarray Scanner, and images were analysed using Feature Extraction software 11.0.0.1 with background correction. Normalization was performed using GeneSpring GX 12.1 software. The raw data was accessible in the online public database (GEO accession: GSE124360).

NF-κB activity assay

NF-κB activity was assessed as previously described (20). Briefly, 1×10^6 HEK-293T cells were cultured in 24-well plates, and each well was transfected with 0.1 μg of an NF-κB luciferase reporter plasmid, 0.1μg of a β-gal expression plasmid (Ambion) and 0.5 μg of a TLR8 overexpression plasmid using Lipofectamine 2000 (Invitrogen); β-gal was used as the transfection control. After 24 h of culture, the cells were stimulated with miRNAs (5μg/ml) complexed with DOTAP for an additional 12 h and assayed via luciferase (Promega, Madison, WI, USA).

Generation of TLR7-KO murine macrophages

To generate TLR7-KO RAW264.7 cells, target sequences were cloned into pLentiCRISPRv2 via *BsmBI* as previously described (21). The target sequences were validated for the function and one target sequence (TLR7 target #1, CACCGACGTGATTGTGG CGGTCAG) was used.

miR-122 pull-down assay and LC-MS/MS

Biotin-anti-miR-122 complementary to human mature miR-122 and biotin-scramble-RNA were synthesized (Genscript), 3'- and 5'-labelled with biotin and dissolved in washing/binding buffer (500 mM NaCl, 20 mM Tris-HCl and 1 mM EDTA, pH7.5) at a final concentration of 20pmol/ml. Biotin-anti-miR-122 and biotin-scramble-RNA were then incubated with streptavidin-coated magnetic beads (New England BioLabs) according to the manufacturer's instructions (13). 40 ml plasma pooled from ten chronic hepatitis patients were used for pull-down assay (SI Appendix, Tables S1). 20 ml plasma samples were pre-treated with DNase I (Takara) and then incubated with biotin-anti-miR-122-coated or biotin-scramble-RNA-coated magnetic beads at 37℃ for 1 h, respectively. Magnets were applied to attract the beads, and the beads-RNA-proteins were then washed with 1 × washing/binding buffer (500 mM NaCl, 20 mM Tris-HCl and 1 mM EDTA, pH7.5) for four times. The proteins were precipitated and diluted in 60μl protein lysis buffer. Finally, the retrieved proteins were measured on SDS-PAGE gels for mass spectrometry by Shanghai Applied Protein Technology (Shanghai, China) as described previously (22).

Statistical Analysis

At least three independent experiments were performed for each set of data, which were presented as the means ± SEMs. Differences are considered statistically significant at $P < 0.05$ using Student's t test, one-way or two-way analysis of variance (ANOVA), and post hoc Bonferroni's multiple comparisons test. All the statistical tests were performed under the open source statistics package R or using GraphPad Prism software 7 (San Diego, CA).

References

1. Fu Y-J, *et al.* (2018) Effects of different principles of Traditional Chinese Medicine treatment on TLR7/NF-kappa B signaling pathway in influenza virus infected mice. *Chinese Medicine* 13.
2. Diao WL, *et al.* (2014) The protective role of myeloid-derived suppressor cells in concanavalin A-induced hepatic injury. *Protein Cell* 5(9):714-724.
3. Maeda S, Kamata H, Luo JL, Leffert H, & Karin M (2005) IKK beta couples hepatocyte death to cytokine-driven compensatory proliferation that promotes chemical hepatocarcinogenesis. *Cell* 121(7):977-990.
4. Jin FF, *et al.* (2017) MiR-26 enhances chemosensitivity and promotes apoptosis of hepatocellular carcinoma cells through inhibiting autophagy. *Cell Death Dis.* 8:13.
5. Zhu D, *et al.* (2013) MicroRNA-17/20a/106a modulate macrophage inflammatory responses through targeting signal-regulatory protein alpha. *Journal of Allergy and Clinical Immunology* 132(2):426-436.
6. Liu Y, *et al.* (2016) Tumor Exosomal RNAs Promote Lung Pre-metastatic Niche Formation by Activating Alveolar Epithelial TLR3 to Recruit Neutrophils. *Cancer Cell* 30(2):243-256.
7. Klaunig JE, *et al.* (1981) MOUSE-LIVER CELL-CULTURE .1. HEPATOCYTE ISOLATION. *In Vitro-Journal of the Tissue Culture Association* 17(10):913-925.
8. Chen X, Jin Y, Hou X, Liu F, & Wang Y (2015) Sonic Hedgehog Signaling: Evidence for Its Protective Role in Endotoxin Induced Acute Lung Injury in Mouse Model. *Plos One* 10(11).
9. Li L, *et al.* (2015) Role of Myeloid-Derived Suppressor Cells in Glucocorticoid-Mediated Amelioration of FSGS. *Journal of the American Society of Nephrology* 26(9):2183-2197.
10. Zhang C, *et al.* (2010) Expression Profile of MicroRNAs in Serum: A Fingerprint for Esophageal Squamous Cell Carcinoma. *Clinical Chemistry* 56(12):1871-1879.
11. Zhu K, *et al.* (2017) Plant microRNAs in larval food regulate honeybee caste development. *Plos Genetics* 13(8).
12. Yin Y, *et al.* (2014) Tumor-secreted miR-214 induces regulatory T cells: a major link between immune evasion and tumor growth. *Cell Research* 24(10):1164-1180.
13. Tang R, *et al.* (2012) Mouse miRNA-709 directly regulates miRNA-15a/16-1 biogenesis at the posttranscriptional level in the nucleus: evidence for a microRNA hierarchy system. *Cell Res* 22(3):504-515.
14. Xie J, *et al.* (2012) Long-term, efficient inhibition of microRNRNA function in mice using rAAV vectors. *Nature Methods* 9(4):403-U123.
15. Fabbri M, *et al.* (2012) MicroRNAs bind to Toll-like receptors to induce prometastatic inflammatory response. *Proceedings of the National Academy of Sciences of the United States of America* 109(31):E2110-E2116.
16. Cai Z, *et al.* (2014) Plasma membrane translocation of trimerized MLKL protein is required for TNF-induced necroptosis. *Nature Cell Biology* 16(1):55-65.
17. Shi J, *et al.* (2014) Inflammatory caspases are innate immune receptors for intracellular LPS. *Nature* 514(7521):187-192.
18. Huebener P, *et al.* (2015) The HMGB1/RAGE axis triggers neutrophil-mediated injury amplification following necrosis. *Journal of Clinical Investigation* 125(2):539-550.
19. van Rooijen N & van Kesteren-Hendrikx E (2003) "In Vivo" Depletion of Macrophages by Liposome-Mediated "Suicide". *Liposomes, Pt C,* Methods in Enzymology, ed Duzgunes N), Vol 373, pp 3-16.
20. Heil F, *et al.* (2004) Species-specific recognition of single-stranded RNA via toll-like receptor 7 and 8. *Science* 303(5663):1526-1529.
21. Jin S, *et al.* (2016) USP19 modulates autophagy and antiviral immune responses by deubiquitinating Beclin-1. *Embo Journal* 35(8):866-880.
22. Qian W, *et al.* (2017) Protein kinase A-mediated phosphorylation of the Broad-Complex transcription factor in silkworm suppresses its transcriptional activity. *Journal of Biological Chemistry* 292(30):12460-12470.

Table S1. The clinical features of the hepatic diseases patients for plasma samples collection.

Case No.	Clinical History	Gender	Age (years)	TNM Stage
1	HCC	male	61	T1NxMx
2	HCC	male	49	T1NxcM0
3	HCC	male	69	T2N0cM0
4	HCC	male	64	T1NxcM0
5	IHCC	female	67	
6	HCC	female	60	T1NxMx
7	HCC	male	52	
8	HCC	male	55	T2NxcM0
9	HCC	male	54	
10	HCC	male	45	T2NxcM0
11	Chronic Hepatitis B hepatitis	male	61	
12	Chronic Hepatitis B hepatitis	male	48	
13	Chronic Hepatitis B hepatitis	female	46	
14	Chronic Hepatitis B hepatitis	female	36	
15	Chronic Hepatitis B hepatitis	female	51	
16	Chronic Hepatitis B hepatitis	female	45	
17	Chronic Hepatitis B hepatitis	female	87	
18	Chronic Hepatitis C hepatitis	male	53	
19	Chronic Hepatitis C hepatitis	male	55	
20	Chronic Hepatitis C hepatitis	male	43	

Table S2. The clinical features of patients for pulmonary effusion samples collection.

Case No.	Clinical History	Gender	Age (year)	
1	Chronic hepatitis with pulmonary effusion	female	60	pulmonary effusion
2	Chronic hepatitis with pulmonary effusion	male	52	pulmonary effusion
3	Chronic hepatitis with pulmonary effusion	male	55	pulmonary effusion
4	Chronic hepatitis with pulmonary effusion	male	54	pulmonary effusion
5	Chronic hepatitis with pulmonary effusion	male	45	pulmonary effusion
6	Chronic hepatitis with pulmonary effusion	male	54	pulmonary effusion
7	Chronic hepatitis with pulmonary effusion	male	31	pulmonary effusion
8	Chronic hepatitis with pulmonary effusion	female	46	pulmonary effusion
9	Chronic hepatitis with pulmonary effusion	female	36	pulmonary effusion
10	Chronic hepatitis with pulmonary effusion	female	51	pulmonary effusion
11	Pneumonia without liver disorder	male	78	pulmonary effusion
12	Pneumonia without liver disorder	female	36	pulmonary effusion
13	Pneumonia without liver disorder	female	51	pulmonary effusion
14	Pneumonia without liver disorder	male	16	pulmonary effusion
15	Pneumonia without liver disorder	male	56	pulmonary effusion
16	Pneumonia without liver disorder	female	33	pulmonary effusion
17	Pneumonia without liver disorder	female	23	pulmonary effusion
18	Pneumonia without liver disorder	male	47	pulmonary effusion
19	Pneumonia without liver disorder	Female	60	pulmonary effusion
20	Pneumonia without liver disorder	male	64	pulmonary effusion

Table S3. List of all primers used in the study.

Gene	Forward Primer Sequence	Reverse Primer Sequence
pre-miR-122	GGAGTGTGACAATGGTGTTTG	TTTAGTGTGATAATGGCGTTTG
miR-122-mut	ACACTCCAGCTGGGTGGAGTGTGACAATGC	
TNF-α	CAGGCGGTGCCTATGTCTC	TTAAAAACCTGGATCGGAACCAA
IL-6	CCACGGCCTTCCCTACTTCA	TGCAAGTGCATCATCGTTGTTC
iNOS	GGCAAACCCAAGGTCTACGTT	TCGCTCAAGTTCAGCTTGGT
Arg-1	TTATCGGAGCGCCTTTCTCAA	TGGTCTCTCACGTCATACTCTGT
IFN-γ	ATCTGGAGGAACTGGCAAAA	TTCAAGACTTCAAAGAGTCTGAGG
Msr2	AAAGAAAGCCCGAGTCCC	TGCCCAAGGAGATAGCAAGA
IL-1	TACCAGTTGGGGAACTCTGC	CAAAATACCTGTGGCCTTGG

Table S4. Complete table of putative miR-122-binding proteins in hepatitis patients' plasma identified by LC-MS/MS (ranked in order peptide count). Proteins were not included in the Table if the peptide count was less than 10.

NO.	Protein	Gene	GO Analysis	Pep Count (scramble-RNA)	Pep Count (anti-miR-122)	Unique PepCount	Cover Percent (%)
1	Alpha-2-macroglobulin	A2M	Calcium-dependent protein binding	0	171	62	61.06
2	Coagulation factor V	F5	Copper ion binding	0	116	54	28.96
3	Alpha-2 globin chain	HBA2	Heme binding	0	75	11	91.55
4	Apolipoprotein A-I, isoform CRA_a	APOA1	lipid binding	0	73	31	85.02
5	Immunoglobulin heavy constant gamma 3	IGHG3	Antigen binding	0	60	15	46.95
6	Spectrin beta chain, erythrocytic	SPTB	Actin binding	0	54	49	27.52
7	Talin-1	TLN1	Actin filament binding	0	48	44	23.93
8	Ankyrin-1	ANK1	ATPase binding	0	47	39	26.58
9	Immunoglobulin heavy constant mu	IGHM	Antigen binding	0	42	20	52.76
10	CP protein	CP	Copper ion binding	0	36	28	29.95
11	Immunoglobulin heavy constant gamma 4	IGHG4	Antigen binding	0	36	11	51.68
12	Haptoglobin	HP	Hemoglobin binding	0	34	22	46.55
13	Inter-alpha (Globulin) inhibitor H2	ITIH2	Serine-type endopeptidase inhibitor activity	0	23	20	21.88
14	Complement component C7	C7	Complement activation	0	21	18	22.18
15	Apolipoprotein A-II	APOA2	Lipid binding	0	21	8	51.88
16	Hemoglobin beta	HBB	Oxygen binding	0	19	6	67.62
17	Afamin	AFM	Vitamin E binding	0	18	15	29.88
18	Hbbm fused globin protein	HBB	Heme binding	0	17	5	51.49
19	Erythrocyte membrane protein band 4.2	EPB42	ATP binding	0	15	13	21.27
20	Immunoglobulin lambda constant 7	IGLC7	Antigen binding	0	14	4	50.94
21	Immunoglobulin kappa variable 3D-20	IGKV3D-20	Antigen binding	0	14	3	27.59
22	Beta-actin-like protein 2	ACTBL2	ATP binding	0	12	7	17.29
23	Alpha-2-antiplasmin	SERPINF2	Protease binding	0	11	8	20.16
24	Vitronectin	VTN	Collagen binding	0	10	8	23.01
25	Serum paraoxonase/arylesterase 1	PON1	Calcium ion binding	0	10	7	20

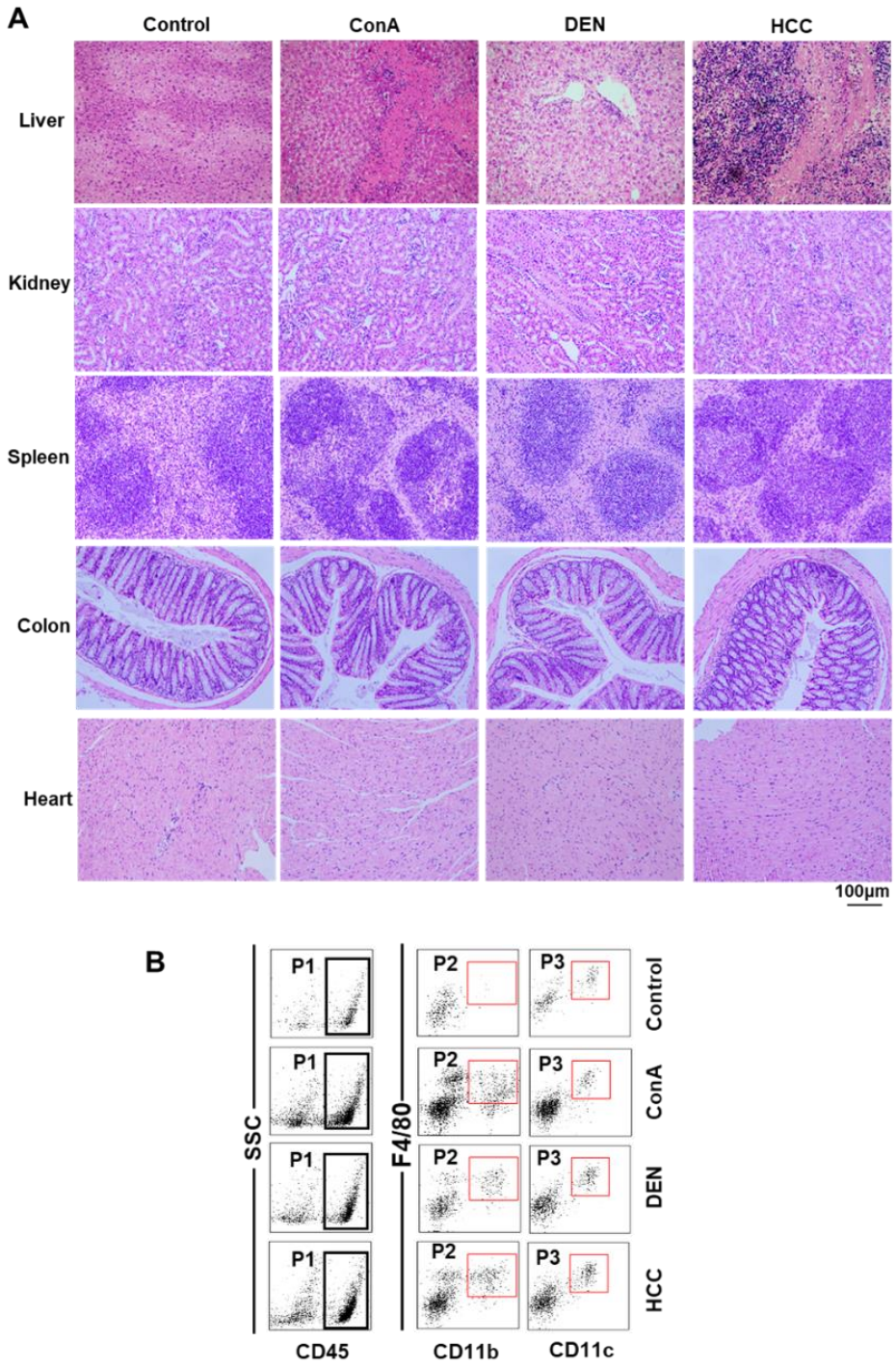

Figure S1. Tissue damage and infiltration of macrophages in mice with active ConA-induced acute hepatitis, DEN-induced chronic hepatitis or orthotopic transplanted HCC. **(A)** Representative H&E staining of mouse liver, kidney, spleen, colon and heart sections. **(B)** Alveolar infiltration of macrophages in mice with active various liver injures (6 mice/group).

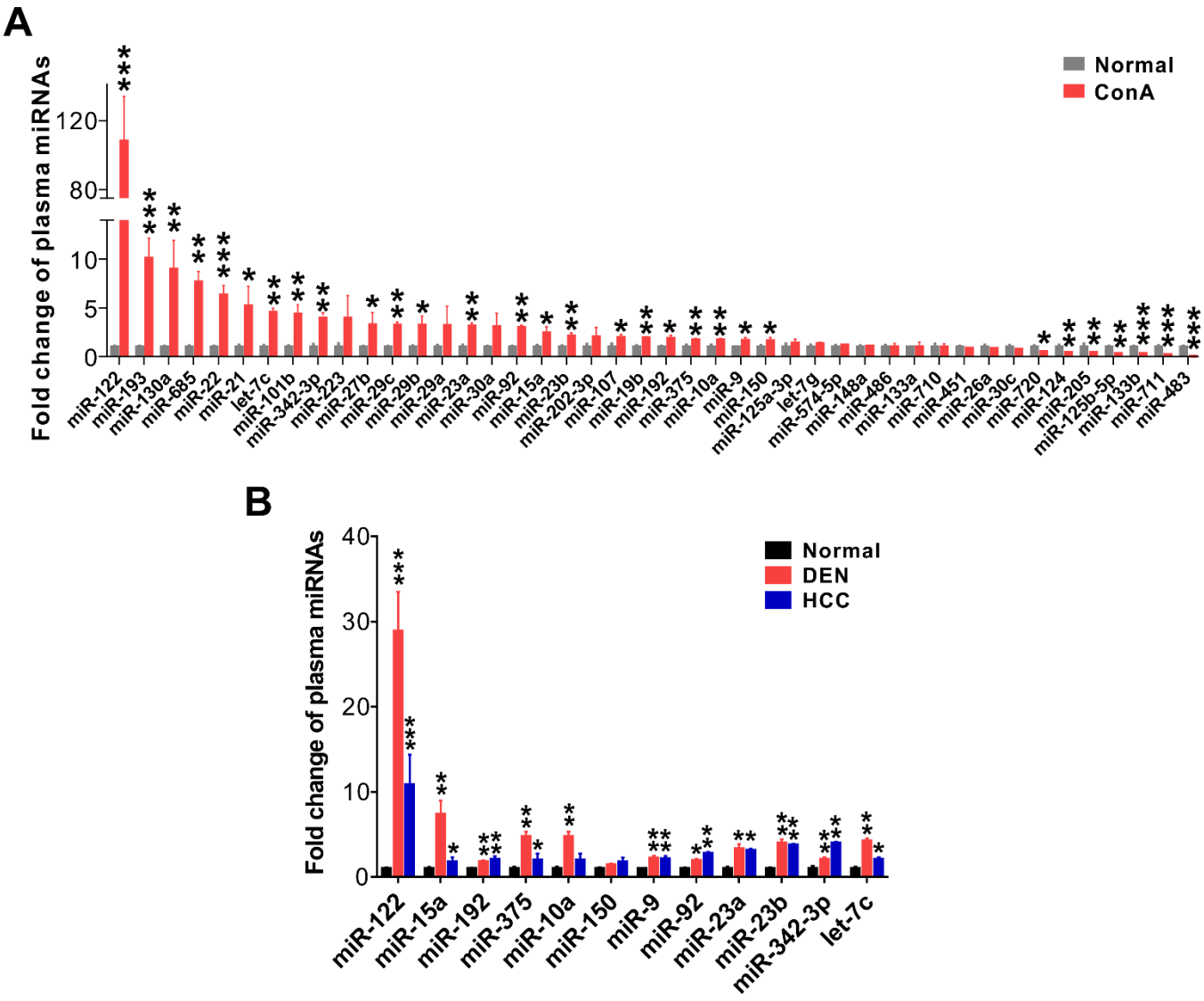

Figure S2. Plasma miRNA expression profile in various mouse models of liver injury**. (A)** Increase of plasma miR-122 levels in mice with ConA-induced acute hepatitis compared to that in normal mice (6 mice/ group, n=3). (B) Increase of plasma miR-122 levels in mice with DEN-induced chronic hepatitis or orthotopic transplanted HCC compared to that in normal mice (6 mice/ group, n=3). Data are presented as mean ±SEM. *, $P < 0.05$, **, $P < 0.01$, ***, $P < 0.001$. Student's two-tailed, unpaired *t*-test (A), or one-way ANOVA followed by Bonferroni's multiple comparisons test (B).

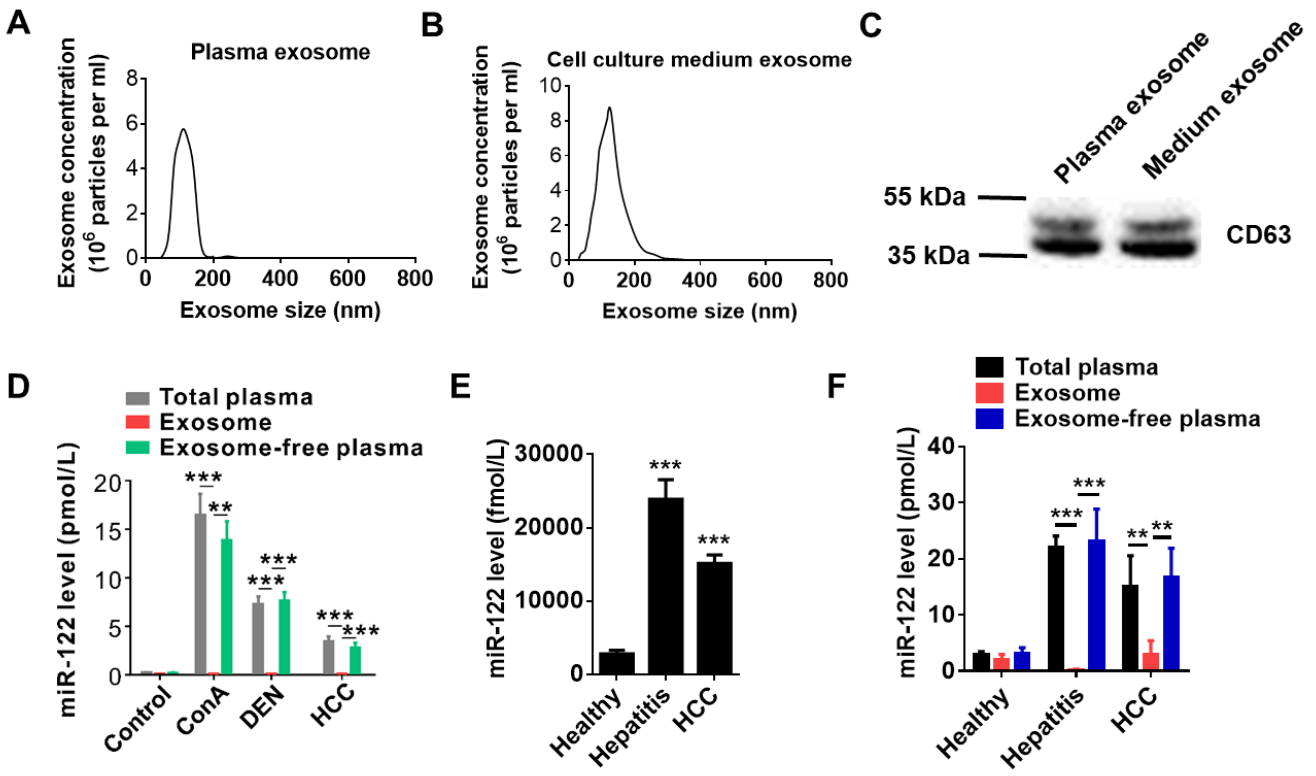

Figure S3. Circulating miR-122 is mainly in exosome-free fraction in mouse models of liver injury and patients with hepatitis or HCC. **(A-C)** Isolated exosomes from plasma and cell culture medium assessed by NTA (A and B) and WB (C). **(D)** Circulating miR-122 released by mouse injured liver cells is mainly in exosome-free fraction. **(E)** Plasma miR-122 levels in 10 healthy donors, 10 hepatitis and 10 HCC patients. **(F)** Circulating miR-122 in patient plasma is mainly in exosome-free fraction. Data are presented as mean ± SEM. **, $P < 0.01$, ***, $P < 0.001$. One-way ANOVA followed by Bonferroni's multiple comparisons test.

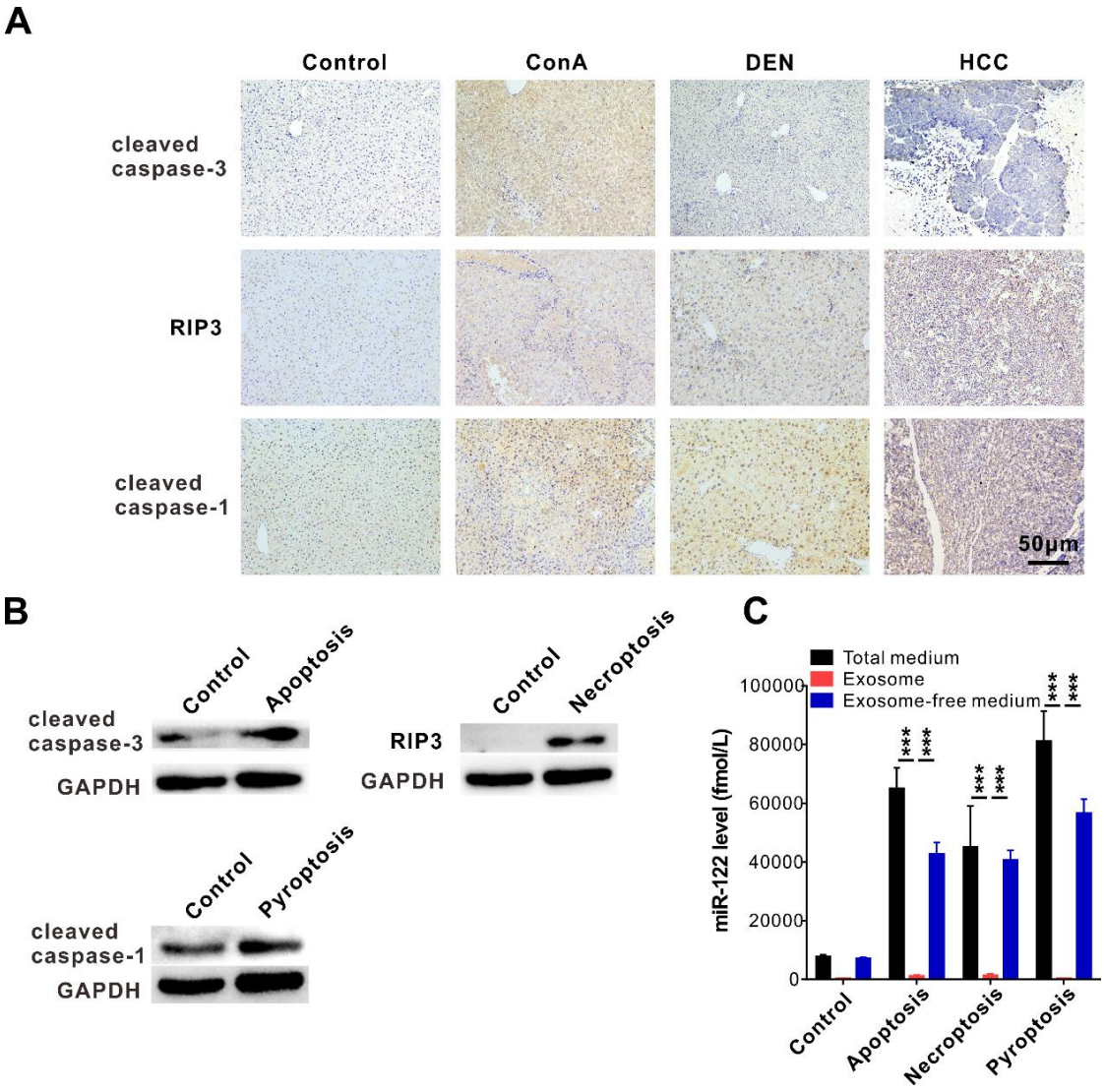

Figure S4. Inflammatory forms of cell death in various liver injures. **(A)** The protein marker of apoptosis (cleaved-caspase3), necroptosis (RIP3) and pyroptosis (cleaved-caspase1) were monitored in liver sections from mice bearing HCC or treated with ConA or DEN. (B) Apoptosis, necroptosis or pyroptosis were induced in cultured primary hepatocytes and assessed by WB. (C) The miR-122 released from various injured hepatocyte were all mainly in exosome-free fraction. Data are presented as mean ± SEM. ***, $P < 0.001$. One-way ANOVA followed by Bonferroni's multiple comparisons test.

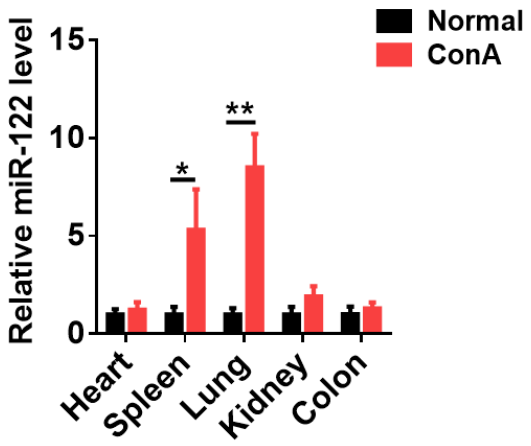

Figure S5. MiR-122 level in various organs from mice with or without active ConA-induced acute hepatitis. Data are presented as mean ± SEM. *, $P < 0.05$, **, $P < 0.01$. Student's two-tailed, unpaired *t*-test.

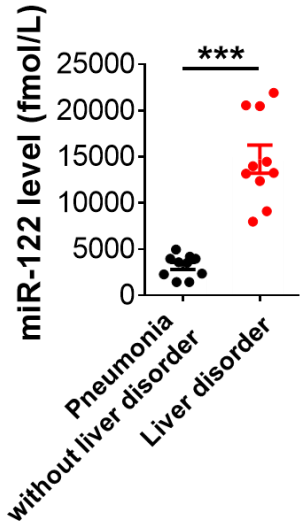

Figure S6. Increased miR-122 level in pulmonary effusion from 10 hepatitis patients compared to that from 10 severe pneumonia patients without liver diseases. Data are presented as mean ± SEM. ***, $P < 0.001$. Student's two-tailed, unpaired *t*-test.

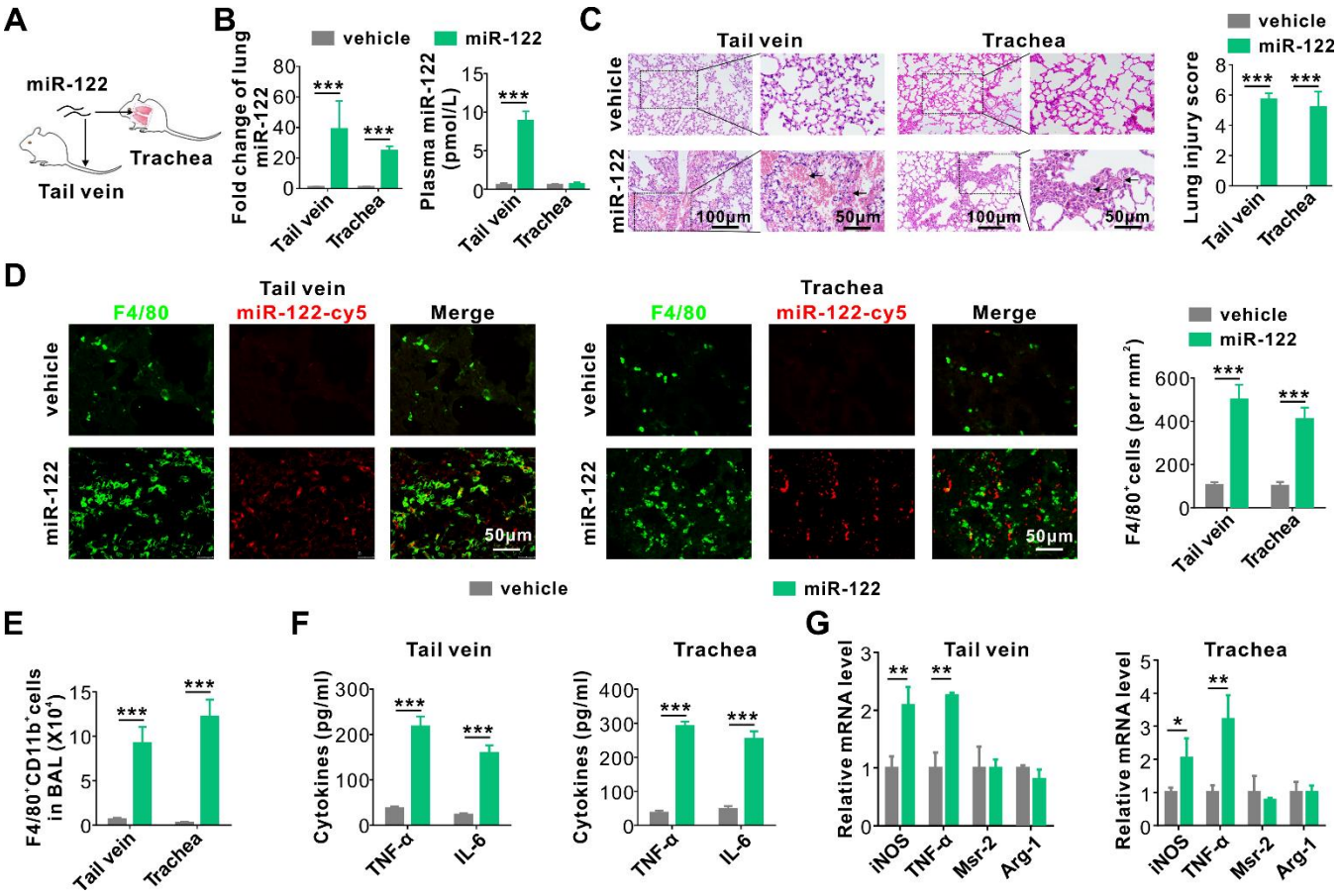

Figure S7. Direct injection of miR-122 via tail vein or respiratory trachea results in inflammatory activation of alveolar macrophages. **(A)** Schematic of experimental design. **(B)** Fold change of miR-122 level in mouse lungs (left) and plasma (right) following direct injection of synthetic miR-122 via tail vein or respiratory trachea, respectively. **(C)** miR-122 injection-induced mouse lung tissue damage quantitated by lung injury score. **(D)** Representative images (left) and statistically analysis (right) of injected miR-122-Cy5 and infiltrated macrophages in lung tissues detected by immunofluorescence (6 mice/group, 3-5 images/mouse). **(E)** FACS analysis of $F4/80^{+}CD11b^{+}$ macrophages in BAL harvested from mice with or without miR-122 injection (6 mice/group, n=3). **(F)** Levels of inflammatory cytokines in BALF from mice with or without miR-122 injection (6 mice/group, n=3). **(G)** Levels of M1 polarization-related gene transcripts in alveolar macrophages from mice with or without miR-122 injection (6 mice/group, n=3). Data are presented as mean ± SEM. *, $P < 0.05$, **, $P < 0.01$, ***, $P < 0.001$. Student's two-tailed, unpaired *t*-test.

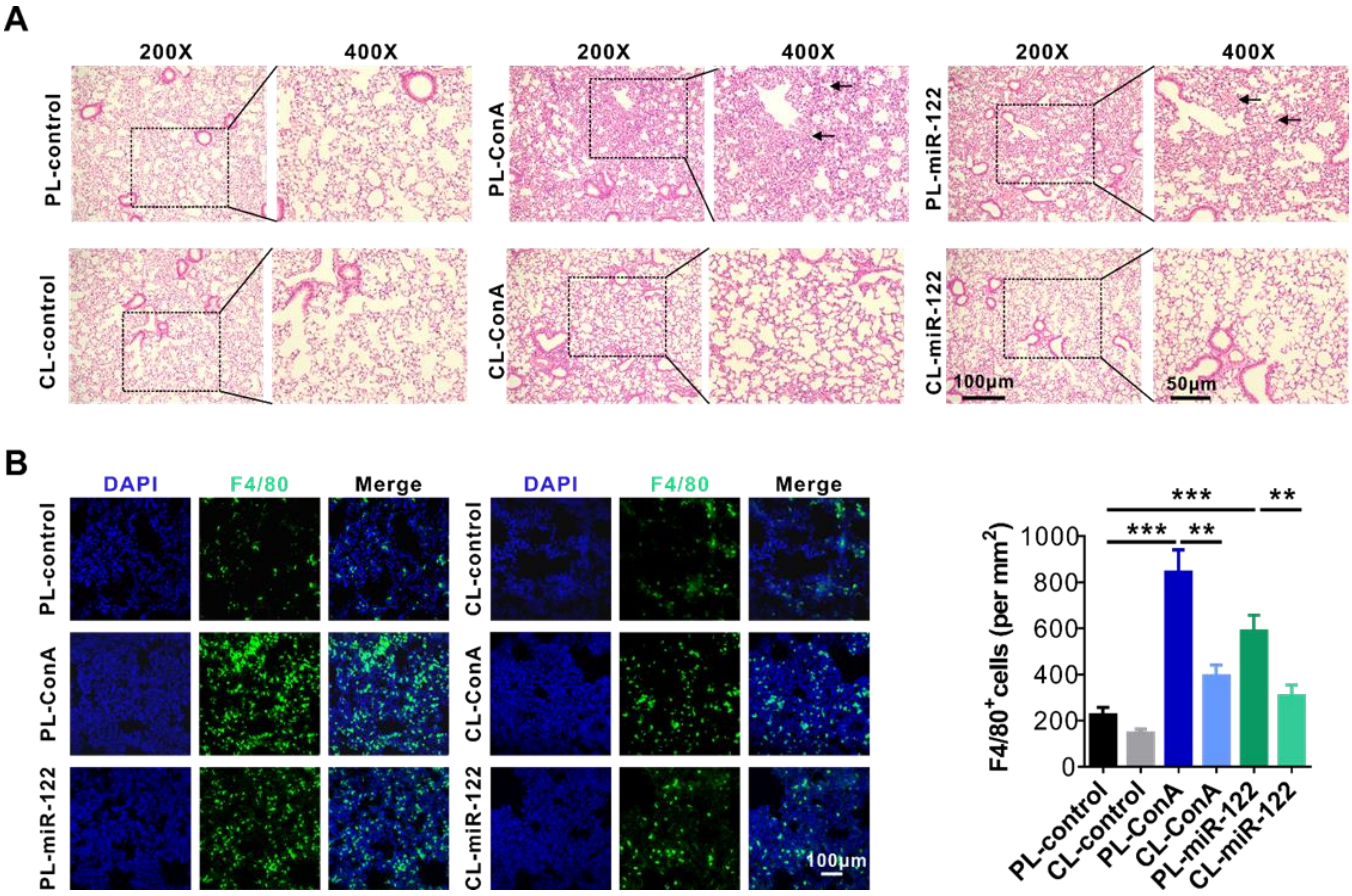

Figure S8. Depleting macrophages attenuates pulmonary inflammation and tissue damage induced by injured liver or circulating miR-122. **(A)** Mouse lung tissue damage analysed by H&E staining. Mice from control group (PL-control) and macrophage-depleted group (CL-control) were injected with ConA (PL-ConA, CL-ConA) or synthetic miR-122 (PL-miR-122, CL-miR-122), respectively. **(B)** Representative images (left) and analysis (right) of $F4/80^+$ macrophage infiltration into mouse lungs (n=6 mice/ group, 3-5 images/ mouse). Data are presented as mean ± SEM. **, $P < 0.01$. ***, $P < 0.001$. One-way ANOVA followed by Bonferroni's multiple comparisons test.

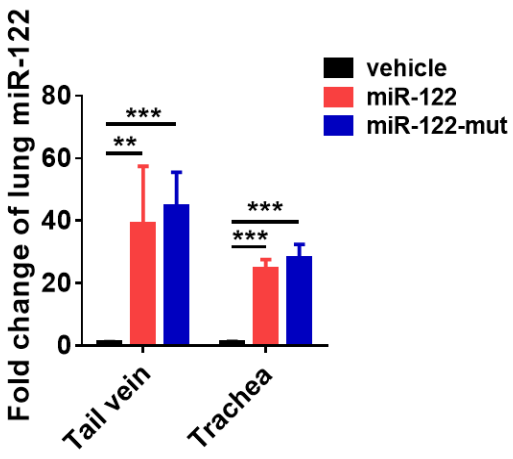

Figure S9. Fold change of miR-122 or miR-122-mut level in mouse lungs before or after miR-122/miR-122-mut injection via tail vein or respiratory trachea, respectively. Data are presented as mean ± SEM. **, $P < 0.01$, ***, $P < 0.001$. One-way ANOVA followed by Bonferroni's multiple comparisons test.

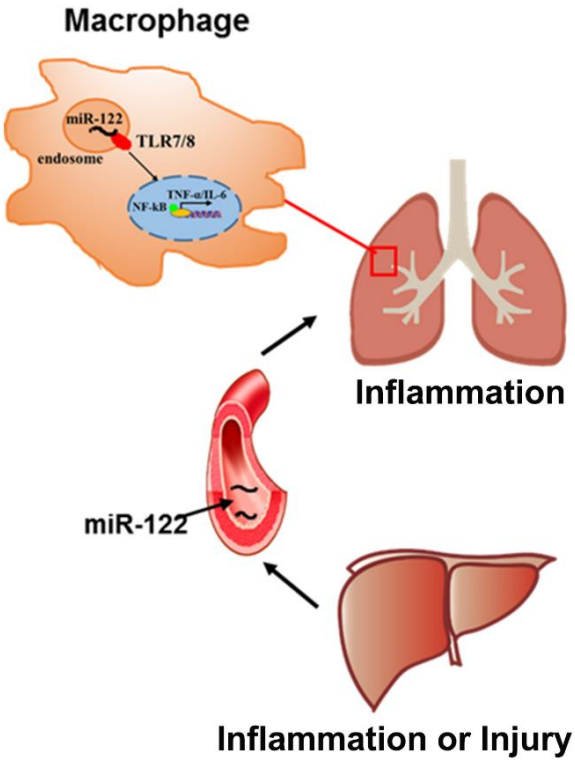

Figure S10. Graphic abstract of pulmonary inflammation induced by injured liver-released miR-122.